Microbiome

RESEARCH Open Access

Allicin enhances urea-N conversion to microbial-N by inhibiting urease activity and modulating the rumen microbiome in cattle

Shiqi Zhang[1], Nan Zheng[1], Shengguo Zhao[1*] and Jiaqi Wang[1*]

Abstract

Background Urea serves as a vital nonprotein nitrogen source in ruminant nutrition, but its efficient utilization is often hampered due to rapid urease activity in the rumen. This study explores the potential of allicin, a garlic-derived compound, as a urease inhibitor to improve urea nitrogen utilization. Enzyme inhibition kinetics and molecular docking were used to identify allicin's interaction sites on urease. Additionally, metagenomic and ^{15}N-urea metabolic flux analyses were conducted to evaluate allicin's impact on microbial populations and urea-N metabolism.

Results Allicin was identified as an inhibitor of ruminal urease, with an IC_{50} of 126.77 ± 1.21 μM. Molecular docking studies have shown that allicin forms hydrogen bonds with key urease residues, leading to the preemption of the urease active site and thus impeding urea binding. In a simulated rumen environment, allicin significantly reduced urea hydrolysis and ammonia production. Furthermore, allicin modified the rumen microbial community by inhibiting *Prevotella* species while promoting the growth of *Ruminobacter* species and *Denitrobacterium detoxificans*. A ^{15}N-urea metabolic flux analysis revealed that allicin facilitated the incorporation of urea-derived nitrogen into microbial amino acids and nucleotides.

Conclusion Allicin effectively inhibits urease activity in the rumen, enhancing the conversion of urea-N into microbial biomass. These findings suggest that allicin has significant potential to optimize urea metabolism in the rumen, offering a novel strategy for improving ruminant nitrogen nutrition.

Keywords Allicin, Rumen microbiome, Urease inhibition, Urea nitrogen, Microbial nitrogen

Background

The limited land and low production efficiency of soybean meal have led to a shortage of protein feed resources in some countries, constraining the growth of the livestock industry [1, 2]. To address this issue, strategies such as partially replacing soybean meal nitrogen with forages containing higher nitrogen content [3, 4] and other protein meals [5] have been explored. Additionally, the development of additives that improve nitrogen utilization efficiency represents another approach to reducing the reliance on soybean meal as a protein source [6]. Urea is a cost-effective alternative that can replace 20–30% of crude protein in cattle and sheep diets. Urea, with 46.7% nitrogen content, offers a significant advantage over soybean meal, which contains only 6.8% nitrogen, making urea approximately 6.8-fold richer in nitrogen [7–9].

*Correspondence:
Shengguo Zhao
zhaoshengguo1984@163.com
Jiaqi Wang
jiaqiwang@vip.163.com
[1] State Key Laboratory of Animal Nutrition and Feeding, Institute of Animal Sciences, Chinese Academy of Agricultural Sciences, Beijing 100193, China

Even in diets without urea supplementation, endogenous urea is recycled to the rumen. The rate of ammonia production from dietary nitrogen in the rumen often exceeds its incorporation into microbial nitrogen, leading to excess ammonia absorption through the rumen wall, followed by conversion to urea in the liver [10]. Although some endogenous urea is recycled to the rumen, where ammonia again becomes available to microbes, the majority is excreted in urine [11]. Urea excreted in urine is rapidly hydrolyzed to ammonium in soils, potentially contaminating watercourses as nitrate and releasing nitrous oxide, a potent greenhouse gas [12]. Therefore, enhancing urea-N utilization in cattle, sheep, and other ruminants is critical not only for reducing soybean meal usage and improving economic efficiency but also for mitigating environmental impact.

One promising approach to improving nitrogen utilization in ruminants is reducing the rate of urea breakdown using urease inhibitors [13]. Allicin, a bioactive compound derived from garlic, has been reported to have bactericidal, immune-modulating, antioxidant, and growth-promoting properties [14, 15]. Allicin has also been shown to inhibit the activities of soil [16] and cuttlebean urease [17]. Our previous research demonstrated that garlic essential oil could slow down the rate of urea hydrolysis and inhibit ammonia nitrogen production [18]. However, the potential of allicin as a urease inhibitor in the rumen remains underexplored. Given that the quaternary structure of ruminal bacterial ureases differs significantly from other environmental ureases [19], the specific mechanism by which allicin inhibits ruminal bacterial urease activity is not well understood. Furthermore, the effects of allicin on the metabolic fate of urea nitrogen in the rumen and its incorporation into microbial nitrogen have not been fully elucidated.

We hypothesize that allicin acts as a competitive inhibitor by binding to the active site of ureases, thereby enhancing the incorporation of urea-N into microbial nitrogen. To test this hypothesis, we employed enzyme inhibition kinetic assays and molecular docking techniques to explore the nature of urease activity inhibition and the binding site of allicin. Additionally, the impact of allicin on microbial populations and nitrogen flux was assessed using metagenomic and metabolic flux analysis.

Methods

Rumen fluid collection and the preparation of rumen bacterial urease crude solution

Ruminal contents were obtained from three Holstein lactating cows (572 ± 24.3 kg, mean ± SD) fitted with rumen fistulae. Fistulated cattle were fed a total mixed ration consisting of (dry matter basis) 17.3% alfalfa hay, 18.7% maize silage, 11.3% soybean meal, 4.2% rapeseed meal, 2.1% cotton aphid, 2.1% puffed soybeans, 4.2% beet pulp, 10.4% whole cottonseed, 25.6% maize, 0.5% salt, and 3.6% premix. The nutritional composition of this ration was as follows: crude protein at 17.84%, ether extract at 2.51%, neutral detergent fiber at 30.11%, acid detergent fiber at 16.30%, and starch at 25.81%. Fistulated cows were fed three times a day. Rumen fluid was collected before morning feeding. Rumen fluid from three cows was mixed, and the rumen contents were filtered through four layers of gauze and then centrifuged at 300 × *g* and 4 °C for 10 min to remove plant particles. The supernatant (50 mL) was then centrifuged again at 12,000 × *g* and 4 °C for 5 min. The supernatant was discarded, and the pellet was resuspended in 50-mL cold 4-hydroxyethyl piperazine ethane sulfonic acid (HEPES) buffer (50 mM, pH 7.5) and centrifuged again at 12,000 × *g* and 4 °C for 5 min. The pellet was resuspended again with 25-mL HEPES buffer and then sonicated with an ultrasonic cell crusher (Nasonic Ultrasonic Technology Co.) at 150-W power for 10 min, with each sonication interval lasting for 6 s with 6-s interruptions. The crude bacterial urease enzyme solution was obtained by centrifugation at 4 °C and 13,000 × *g* for 10 min.

Maximum half-inhibitory concentration (IC_{50}) values of allicin

The enzymology assay to characterize the kinetics of inhibition of ruminal bacteria urease activity by allicin natural was performed in 96-well plates using Nessler reagent spectrophotometry [20]. Urea was dissolved to 12 mg/L using 50-mM HEPES. Allicin (≥ 97% HPLC, Shanghai Yuanye Biotechnology Co., China) was solubilized using 10% dimethyl sulfoxide (DMSO, DMSO: distilled water = 1:9 w/w, Thermo Fisher Scientific, USA) to a 2500-μM stock solution and then subjected to nine gradients of doubling dilution (2500.00, 1250.00, 625.00, 312.50, 156.25, 78.13, 39.06, 19.53, and 0 μM) for the allicin working solution. In the allicin assay, 40 μL of allicin working solution (final concentrations of 0 (10% DMSO), 3.91, 7.81, 15.63, 31.25, 62.50, 125.00, 250.00, and 500.00 μM) and 40 μL of crude ruminal urease solution were added, and after incubation, for 10 min at room temperature, 100 μL of urea solution (final concentration of 10 mM) was an addition. In the allicin control assay, the urea solution was replaced with HEPES 100 μL (to reduce the interference of other ions), and the procedure was the same as that of the allicin assay group. In the ruminal urease assay, 40 μL of crude urease solution and 40 μL of HEPES were added and incubated at room temperature for 10 min before adding 100 μL of urea solution (final concentration of 10 mM). The urea solution was replaced with HEPES 100 μL in the ruminal urease control group, and the procedure was the same

as that of the ruminal urease assay group. After 30 min of incubation at 37 °C, 10 μL of 50% w/v Rochelle salt solution was added to the mixture to minimize interference of non-NH_4^+ ions, followed by 10 μL of Nessler reagent. The mixture was allowed to react for 10 min [21], and then the absorbance of each well representing the ammonia concentration was measured at 420 nm using an enzyme calibrator (Varioskan LUX, Thermo Scientific). Three replicates were performed for each concentration. Absorbance values (OD) for each treatment were calculated as residual activity (%) of rumen bacterial urease: residual activity (%) = [(OD of allicin group — OD of the allicin control group)/(OD of rumen urease group — OD of rumen urease control group)] × 100 [22]. Residual activity and allicin concentration curves were fitted using GraphPad Prism (version 9, GraphPad, USA), and IC_{50} were calculated.

Inhibition of urease kinetic parameters by allicin

Responses to urease activity change with varying urea concentrations (0, 3.125, 6.25, 12.50, 25.00 mM) in the presence or absence of allicin (0, 125, 250, and 500 μM) using nonlinear regression, and linear fitting of Lineweaver–Burk plots was analyzed with GraphPad Prism. Specifically, Michaelis–Menten enzyme kinetics were applied to determine the kinetic parameters, including the Michaelis constant (Km) and maximum velocity (Vmax). The assay was performed as described above in the "Maximum half-inhibitory concentration (IC_{50}) values of allicin" section.

Molecular docking

The rumen bacterial urease structure was modelled using a previous homology reported by Zhang et al. [23], and the rumen microbial urease gene cluster was downloaded from the NCBI GenBank database (www.ncbi.nlm.nih.gov/genbank/) with accession numbers MN660246 and MN660252.

Urease protein crystals underwent a series of processes using Schrödinger software (Maestro 13.1), which included protein preprocessing, optimizing H-bond assignments, regenerating the native states of ligands, minimizing protein energy, and removing water molecules through the Protein Preparation Wizard module. The 2D structures of allicin and urea were prepared, and all their 3D chiral conformations were generated using Schrödinger's LigPrep module. For the protein crystal structure without natural ligands, the optimal binding site was identified with the SiteMap module, and the Receptor Grid Generation module was used to define the most appropriate enclosing box for obtaining the protein's active site. Molecular docking of urea to the protein's active site was performed using high-precision XP docking, and this process was repeated for the protein already complexed with urea. Allicin was then docked into the active site of the urea-bound protein, also with high-precision XP docking, where lower docking scores indicated reduced Gibbs binding energy and greater stability. Finally, the active sites of the two compound-protein complexes were analyzed using MM-GBSA calculations, with lower MMGBSA dG Bind values signifying higher ligand–protein binding stability.

Microbial fermentation in a rumen simulation system

The in vitro fermentation was cultured using 100-mL cell culture bottles. The fermentation system consisted of 22 mL of filtered rumen fluid (see the "Rumen fluid collection and the preparation of rumen bacterial urease crude solution" section for treatment) and 43 mL of anaerobic medium. The anaerobic medium consisted of mg/L: $CaCl_2$ 6.1, KH_2PO_4 228.0, NaCl 45.6, $MgSO_4{\cdot}7H_2O$ 9.5, $NaHCO_3$ 500, and L-cysteine 50, prepared under O_2-free CO_2 [24]. Each bottle contained 1-g dry matter of feed sample (8% soybean meal, 15% corn meal, 10% alfalfa hay, 65% corn silage, 2% premix, DM basis; nutritional levels are as follows: acid detergent fiber 25.69%, neutral detergent fiber 42.30%, crude protein 11.75%) sealed in fiber digestive bags (aperture: 0.5 mm, China Agricultural University, China). Allicin was dissolved in 10% DMSO to prepare different concentrations. The final concentrations of allicin in the rumen culture were 0, 1, 2, or 4 mM, with all treatments containing 650-μL 10% DMSO. A total of five fermentation bottles were allocated to each treatment group. The rumen culture contained 16.7-mM urea. Bottles were sealed under O_2-free CO_2 and incubated in a shaking water batch for 24 h at 39 °C at 120 rpm. No simulation of the nitrogen cycle was performed, simply a static fermentation. The gas pressure was measured, and both gas and incubation broth samples were collected at 0, 2, 4, 6, 12, and 24 h. Incubation broth samples were mixed with 25% (*m*/*V*) metaphosphoric acid solution in a 1:1 (*V*/*V*) ratio. The in vitro fermentation uses the static culture method for three batches of culture on three consecutive days. The fermentation broth samples were mixed 1:1:1 (*V*/*V*/*V*) and used for the assay.

Gas pressure was measured with a digital manometer (ConST, Beijing, China), and gas production was calculated according to Liu et al. [25]. Incubation samples (0.5 mL) were collected for determination of urea, ammonia nitrogen (NH_3-N), and volatile fatty acids (VFAs). VFAs were determined by gas chromatography using 4-methyl-N-valeric acid as an internal standard [26]. NH_3-N was determined using an alkaline sodium hypochlorite-phenol spectrophotometric method [27].

Urea concentration was determined using a urease kit (Nanjing Jianjian Bioengineering Institute, China).

Metagenomic analysis microbial composition and function

Total DNA was extracted from the in vitro rumen incubation broth using the cetyltrimethylammonium bromide method [28], and the quantity and quality of DNA were assessed using NanoDrop One (Thermo Scientific, MA, USA). Sequencing library construction was provided by the MGIEasy kit (BGI, China) and using the 2×100-bp read length of the BGISEQ-500 platform. Quality control analyses were performed using TrimGalore software (0.4.1) [29], explicitly removing reads that were less than 50 bp in length and had an average base mass of less than 20. Host-contaminated sequence data for dairy cows, maize, soybean, and alfalfa were eliminated using BMTagger (v.1.1) [30]. Taxonomic classification was performed using Kraken 2 software [31] against the GTDB-r89 database [32]. High-quality reads from each sample were assembled using MEGAHIT (v.1.1.1) [33]. The acquired MAGs were integrated using the MetWRAP [30]. Integrity and contamination of the MAGs were assessed using CheckM (v.1.0.7) [34, 35]. Eventually, there were 72 MAGs with > 80% completeness and < 5% contamination that were kept for predicting open reading frames in Prodigal (v.2.6.3) [36]. Filtered MAG abundance was analyzed using the metaWRAP software and functionally annotated with eggNOG (v.2) [37]. The relative abundance and diversity of the rumen microbiota were analyzed using the MicrobiomeAnalyst website, where principal component analysis (PCA) and partial least squares discriminant analysis (PLS-DA) analyses at the species level were performed [38]. The differences in the compositional structure of the rumen microflora at the strain level and tagged metabolomic data were analyzed by PCA and PLS-DA in MetaboAnalyst (version 5.0) [39]. The abundance of different functional bacteria was log-transformed. $p < 0.05$ was considered significant. PLS-DA analysis screens for variants with a threshold value of VIP (variable projection importance) ≥ 1.

Urea-N utilization efficiency

In vitro, ruminal incubations which are similar to those described in the "Microbial fermentation in a rumen simulation system" section were conducted. Diet formulation and addition operations are the same as described in the "Microbial fermentation in a rumen simulation system" section. Rumen fluid is obtained and processed as described in the "Rumen fluid collection and the preparation of rumen bacterial urease crude solution" section. A total of three groups of four replicates each were divided into the non-enriched urea group ($^{14}N^{14}N$-urea, Shanghai Yuanye Bio-Technology Co., Ltd., China, 16.7-mM final concentration), the enriched urea control group [$^{15}N^{15}N$-urea (99.08% ^{15}N APE, Shanghai Engineering Research Centre for Stable Isotopes, China), 16.7-mM final concentration], and the allicin group [$^{15}N^{15}N$-urea (99.08% ^{15}N APE, Shanghai Engineering Research Centre for Stable Isotopes, China), 16.7-mM final concentration, and allicin, 2-mM final concentration)]. Incubations were performed for 12 h at 39 °C and 120 rpm.

At the end of the incubations, two 10-mL aliquots of mixed incubation fluid (aliquots from three batches of fermentation) were taken and transferred into a 15-mL centrifuge tube (Suzhou Sentinel Biotechnology Co., China). Before sample division, feed particles were removed by centrifugation at 300 x g at 4 °C. The fluid of one tube (tube A) was centrifuged at 12,000×*g* for 10 min, the supernatant was discarded, and the pellet was washed three times with phosphate buffer saline (PBS). Then, the resulting pellet of microbial cells and plant particles was dried at 70 °C and weighed, because of partial sampling, and any pellet weights had to be converted from 10-mL aliquots to a total volume of 65 mL for ^{15}N isotope abundance determination and calculation. Another tube (tube B) was filled with 0.6 mL of PBS and then frozen and thawed three times with liquid nitrogen. After the last thawing, zirconium grinding beads (1 mm, 200 µg) were added and ground twice on ice for 1 min each time and then mixed well. After centrifugation at 10,000×*g* for 10 min at 4 °C, supernatant was obtained (tube C). The 0.2 mL of the supernatant (tube C) was taken, and the proteins were determined by Kjeldahl nitrogen determination and recorded as free microbial nitrogen. A 0.2-mL aliquot of supernatant (tube C) was mixed with 0.8-mL methanol and centrifuged at 12,000×*g* for 10 min. The supernatant was used to determine ^{15}N-labelled nitrogen-containing metabolite levels (non-targeted metabolic fluxes) by LC/MS/MS and to correct ^{15}N-labelled nitrogen-containing metabolite levels by using the Pierce™ BCA Protein Assay Kit (Thermo Fisher Scientific, USA).

Microbial total N% and ^{15}N abundance were detected using a Vario PYRO cube elemental analyzer in conjunction with an ISOPRIME-100 stable isotope mass spectrometer (Elemental Microanalysis Co., UK). The percentage of ^{15}N-urea incorporated into free microbial ^{15}N was defined as urea-N utilization efficiency and was calculated using the following equation:

$$Urea-N\ utilization\ efficiency(\%) = [(A_1 \times N_1 \times W_1)/(A_2 \times N_2 \times W_2)] \times 100$$

Where A_1 is the ^{15}N abundance in the centrifugation pellet of microbial cells plus undigested plant residues minus the unlabeled control, ^{15}N abundance is the

microbial cell ^{15}N abundance, W_1 is the centrifugation pellet of microbial cells plus undigested plant residues, N_1 is the percentage of N in the tube A sample (%), A_2 is the added urea ^{15}N abundance (99%) divided by the unlabelled control ^{15}N abundance, and W_2 is the added urea weight and N_2 is nitrogen content of $^{15}N^{15}N$-urea (46.7%).

^{15}N-urea metabolic flux

Untargeted ^{15}N-urea metabolic flux analysis was conducted as described previously [40]. Briefly, polar metabolites were extracted from 50 μL of the supernatant sample obtained from tube B using 200-μL ice-cold methanol containing phenylhydrazine for derivatization. After derivatization and centrifugation, the clean supernatant was dried. The dried extract was reconstituted for LC–MS/MS analysis. Separation was achieved using a reverse-phase chromatography column. LC–MS/MS analyses were conducted using an information-dependent acquisition model [39]. In reverse-phase chromatography, polar metabolites were separated using a Waters ACQUITY HSS-T3 column (3.0 × 100 mm, 1.8 μm). Data acquisition and processing were handled using Analyst® TF 1.7.1 Software (AB Sciex, Concord, ON, Canada), with ion identities confirmed through Metabolites database (AB Sciex, Concord, ON, Canada) comparisons and standard references [41]. Internal standards were added for metabolite quantification, and peak areas were normalized accordingly. Automated algorithms were used to select internal standards for quantitation based on minimal coefficients of variation [42, 43].

Statistical analysis

In vitro fermentation data were analyzed using SAS 9.4, where data from different time points were analyzed using the MIXED model. Time and treatment are fixed effects. A Tukey–Kramer test was used for multiple comparisons of differences. Linear and quadratic effects analysis was performed using orthogonal polynomials. Microbial urea-N utilization and free microbial nitrogen data were analyzed using *t*-test. $p < 0.05$ was defined as having a significant difference.

Results

Inhibition of allicin

Allicin inhibited ruminal urease activity in vitro with an $IC_{50} = 126.77 \pm 1.20$ μM (Fig. 1A, $R^2 = 0.976$). The Michaelis–Menten kinetic analysis indicated that both Km and Vmax of ruminal bacterial urease decreased with increasing concentrations of allicin (Fig. 1B). Specifically, as allicin concentration increased from 125 to 500 μM, Km decreased from 1.601 to 1.382 mM, and Vmax decreased from 17.47 to 16.13 mM/min. These results indicate that allicin exerts an inhibitory effect on urease activity by reducing both substrate affinity (Km) and maximum reaction velocity (Vmax), leading to a stable Vmax/Km ratio of 11.26 ± 0.312.

Molecular docking

Molecular docking and MM-GBSA analysis revealed that allicin binds to urease, forming a ternary complex with urea and urease (Fig. 1C, D). Allicin interacts with the Ni ion-linked H_2O^{373} and amino acid residue ARG^{1336} at the active center of urease. In contrast, urea forms hydrogen bonds with residues ALA^{1224}, GLU^{1220}, and GLU^{1252} of urease. The XP GScore for the allicin-urease complex was − 3.137, with an MM-GBSA value of 1.68 kcal/mol, indicating stable binding. The ternary complex (allicin-urease-urea) demonstrated even lower free energy, with an XP GScore of − 3.315 and an MM-GBSA value of − 2.490 kcal/mol (see Additional file 1). This suggests that allicin likely inhibits urease activity via an anticompetitive mechanism, as supported by enzyme kinetics data.

Changes of rumen fermentation

During rumen fermentation, urea content decreased over time, with the 1-mM, 2-mM, and 4-mM allicin groups showing significantly higher urea levels than the control at 2 and 4 h of fermentation ($p < 0.05$) (Fig. 2A). Conversely, NH_3-N levels increased over time, with allicin-treated groups showing significantly lower NH_3-N levels at 2 h ($p < 0.05$) (Fig. 2B). This indicates that allicin slows down the rate of rumen urea degradation. Additionally, gas production was significantly lower in the 4-mM allicin group at 2 and 4 h ($p < 0.05$) (Fig. 2C). VFAs production was significantly higher in the 4-mM allicin group at 24 h, driven by increases in acetic, propionic, and butyric acids and decreases in valeric and isovaleric acids (Fig. 2D, E).

Ruminal bacterial community composition

Allicin affected the microbial diversity in the rumen fermentation, although no significant difference was observed in the Shannon index across the groups at the genus level ($p > 0.05$) (Fig. 3A). Beta-diversity analysis, however, showed significant differences between the allicin-treated groups and the control at the genus level ($p < 0.05$) (Fig. 3B). Among the top 20 most abundant bacterial species, *Prevotella* sp. was the most prominent, but its relative abundance decreased with allicin treatment, while *RC9* sp. and *Ruminobacter* sp. increased (Fig. 3C, D).

Metagenome sequencing generated a total of 405.06 Gb of data (mean ± SD: 20.25 ± 2.42 Gb, maximum 23.8 Gb, minimum 16.7 Gb). A total of 73 rumen microbial MAGs

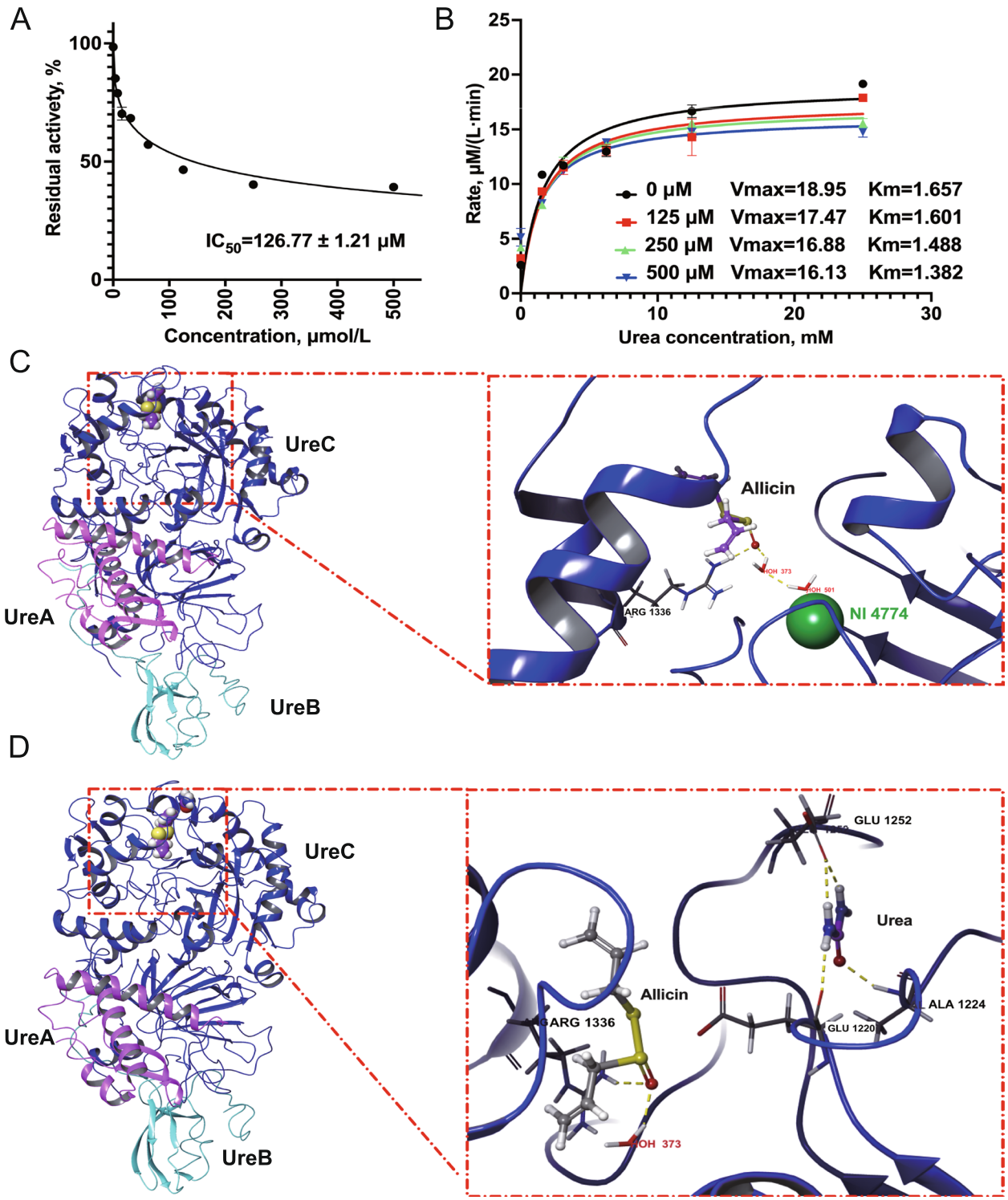

Fig. 1 Kinetic parameters of allicin inhibition of rumen bacterial urease and schematic model of binding to rumen bacterial urease. **A** Residual activity of rumen bacterial urease about allicin concentration. **B** The plot of residual urease activity versus urea concentration in the absence (black ●) and presence of 125 mM (red ■), 250 mM (green ▲), and 500 mM (blue ▼) allicin. The equation is the Michaelis–Menten model [$Y = \mathrm{Vmax} \cdot X/(\mathrm{Km} + X)$], where Y is the reaction rate and X is the substrate concentration. The data were expressed as mean ± SEM. **C** The 2D and 3D plots of allicin-ruminal urease protein docking. **D** A 2D and 3D plots of urea-allicin-ruminal urease protein docking, and the light yellow dotted line represents the hydrogen bond. The urease genes can be divided into structural genes UreA (pink), UreB (light blue), and UreC (dark blue), with the active pocket being at UreC

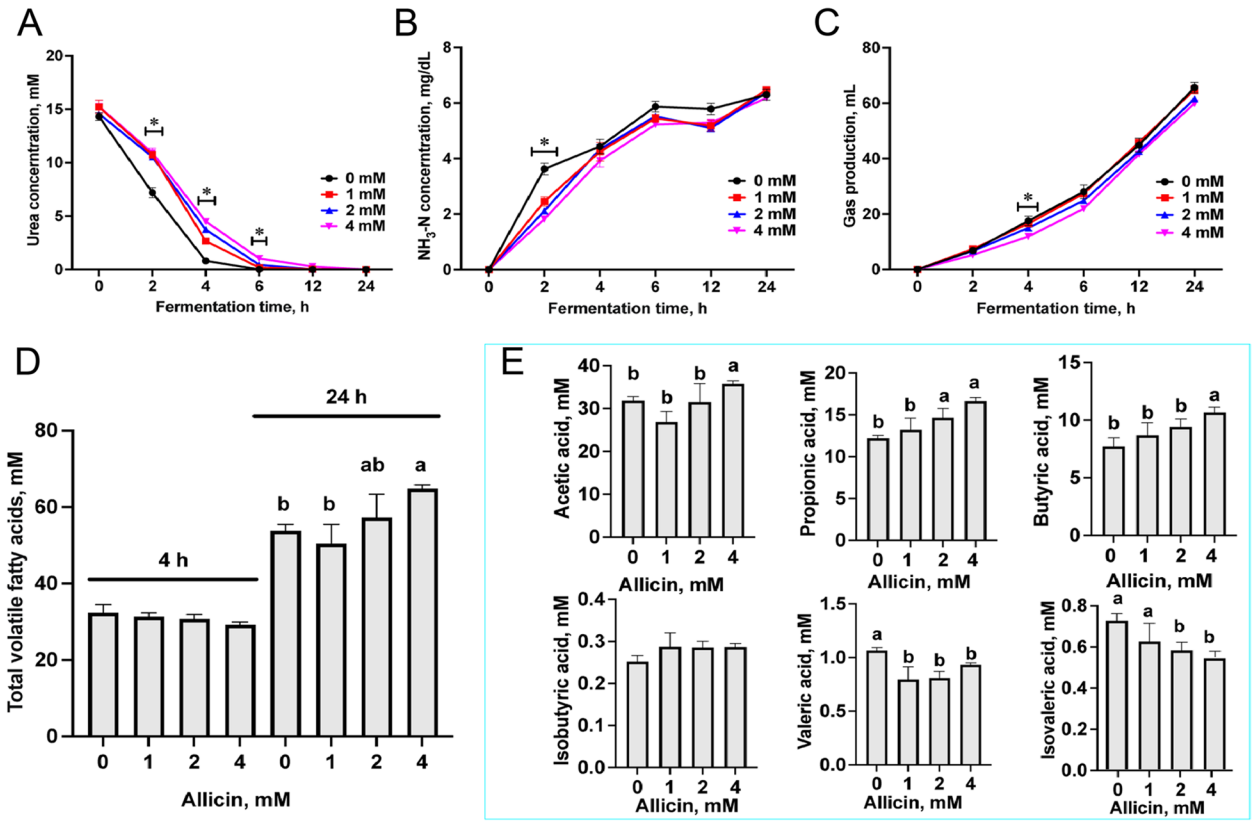

Fig. 2 Effect of allicin on urea nitrogen-related fermentation parameters in the rumen in vitro. Urea nitrogen-related fermentation parameters include urea (**A**), NH_3-N (**B**), gas production (**C**) and volatile fatty acid concentration (**D**). The data were expressed as mean ± SEM. Total volatile fatty acids at 24 h of fermentation include acetic acid, propionic acid, butyric acid, isobutyric acid, valeric acid, and isovaleric acid (**E**). The data were expressed as mean ± SEM. *and a and b represent a significant difference in the difference between treatments not used at this time point ($p < 0.05$)

(completeness mean ± SD: 90.13 ± 5.19%; contamination mean ± SD: 2.12 ± 1.43%) were obtained (Fig. 4A), of which 2 MAGs were archaea and 71 were bacteria (see Additional file 2). A more significant difference in the abundance of MAGs was observed between different groups (Fig. 4B). After PLS-DA analysis, MAG.49 (*D. detoxificans*), MAG.37 (*RC9* sp.), MAG.16 (*Ruminobacter* sp.), MAG.46 (*Denitrobacterium* sp.), MAG.43 (*RC9* sp.), MAG.72 (*Bifidobacterium globosum*), MAG.42 (*F082* sp.), MAG.48 (*RC9* sp.), and MAG.54 (*UBA6985* sp.) were the top changed MAGs (Fig. 4C). Among them, with increasing allicin levels, MAG.49 (*D. detoxificans*), MAG.72 (*B. globosum*), and MAG.37 (*RC9* sp.) abundance increased, and MAG.45 (*Prevotella* sp.) abundance decreased (Fig. 4D).

Urea nitrogen metabolic flux

A total of 55 nitrogenous metabolites were detected using LC/MS/MS, with 45 showing ^{15}N labelling. Notably, 50% of ^{15}N-labelled molecules were found in nicotinamide adenine dinucleotide (NAD), nicotinamide adenine dinucleotide phosphate (NADP), uridine diphosphate N-acetylglucosamine (UDP-GlcNAc), and N-acetyl-L-aspartic acid (Fig. 5A). These metabolites were involved in pathways such as purine metabolism, ammonia recycling, and the urea cycle (Fig. 5B). It was suggested that $^{15}N^{15}N$-urea is involved in microbial growth and metabolism, e.g., purine metabolism or hypoxanthine metabolism via glutamine metabolism, aspartic acid metabolism via glutamate-arginine, and amino sugar metabolism and pyrimidine metabolism via beta-alanine metabolism (Fig. 6).

Allicin improved urea-N utilization efficiency and free microbial nitrogen ($p < 0.05$), and it also increased the flux of rumen urea-N to microbial-N ($p < 0.05$) (Fig. 7A). A non-targeted metabolomic profile of the ^{15}N-containing metabolites showed a clear distinction between the allicin and the control group (Fig. 7B). PLS-DA analysis revealed 12 changed metabolites by allicin, which is involved in amino acid metabolism, amino sugar metabolism, urea cycle, pyrimidine metabolism, microbial metabolism, and other pathways (Fig. 7C, D). The allicin promoted urea-^{15}N flux

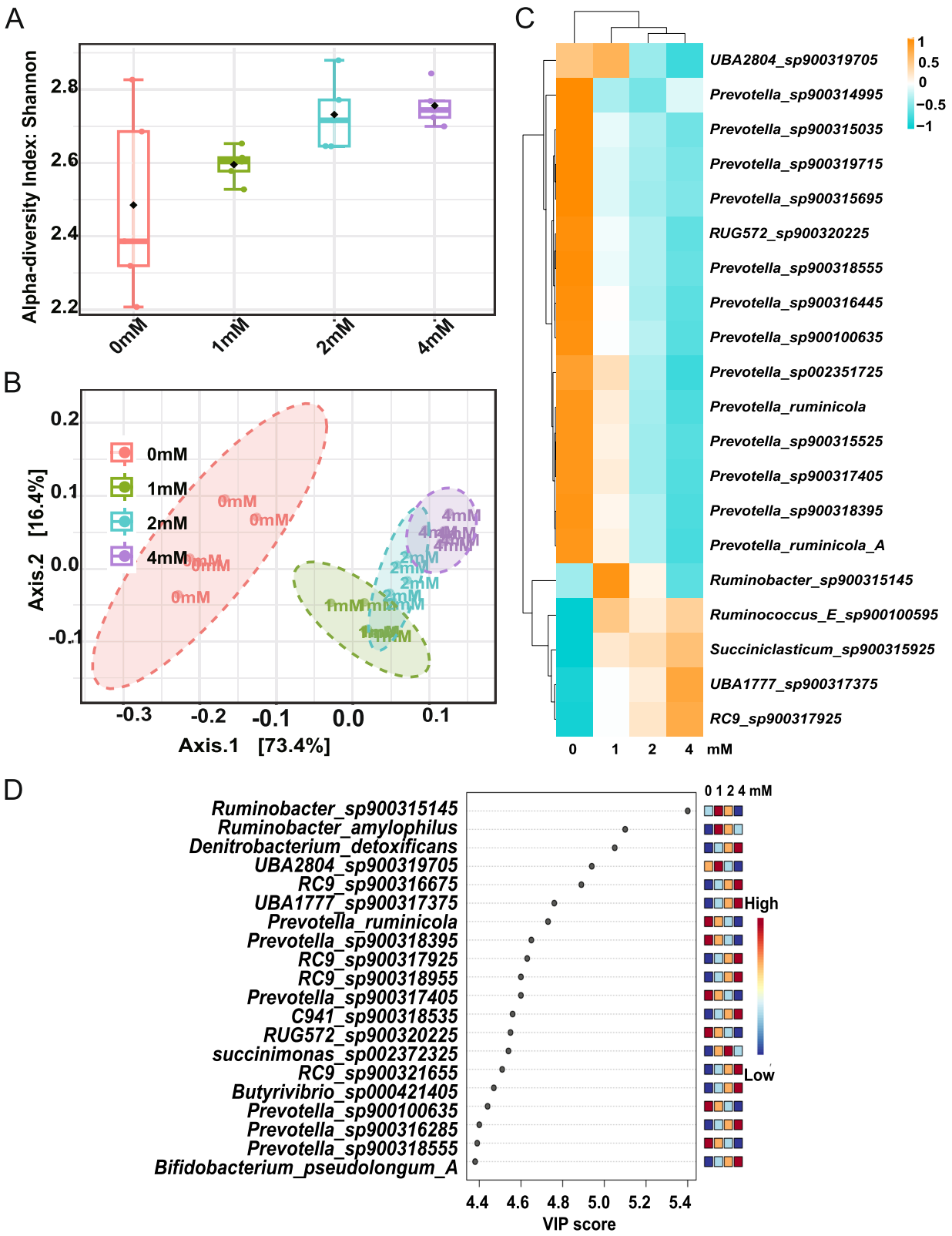

Fig. 3 Ruminal microbial community composition. **A** Alpha-diversity Shannon index chart at the genus level. **B** The effect of allicin on the structure of the rumen bacterial population at the genus levels. In the legend, 0 mM represents the control, and 2 mM, 4 mM, and 8 mM represent the doses of allicin. **C** The top 20 relative abundance of rumen microflora at species levels. **D** LEfSe analyses of the four groups. The *x*-axis indicates LDA scores, i.e., the extent of the effect of the different bacterial genera. The *y*-axis indicates the bacteria that differed significantly among the groups

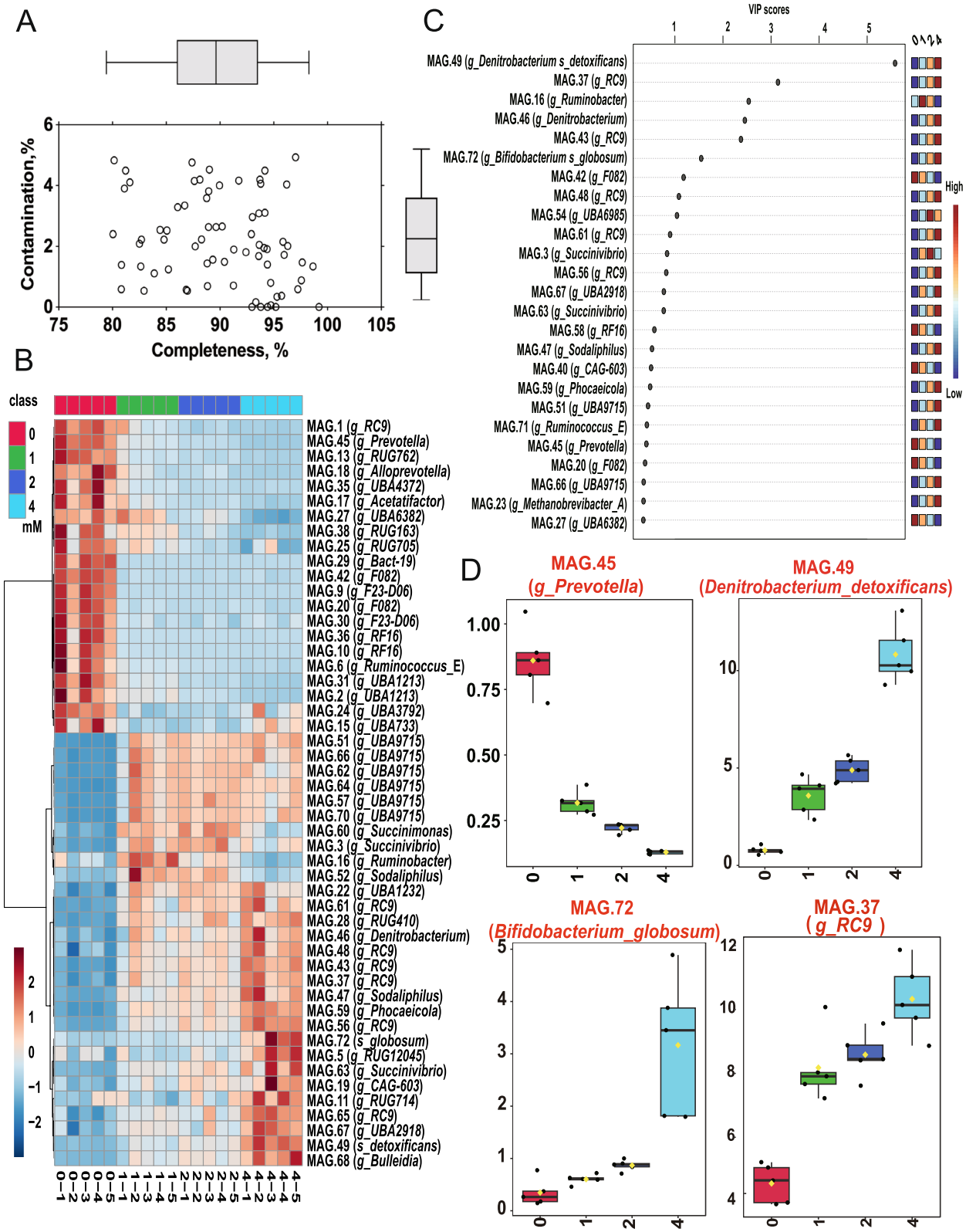

Fig. 4 Effect of allicin on the relative abundance of rumen bacteria strains. **A** MAG's contamination and completeness. **B** Changes in abundance of the top 50 strains at different allicin concentrations. **C** The top 15 species according to VIP values analyzed by PLS-DA. **D** Effect of allicin on the relative abundance of target bacterial strains

into uridine 5′-monophosphate (GMP), UDP-GlcNAc, adenosine 5′-monophosphate (AMP), uridine 5′-monophosphate (UMP), L-alanine, and guanosine (Fig. 7E, F, G, H, I, J).

Discussion

Ruminal bacterial urease is vital for the utilization of nonprotein nitrogen feeds, but its high activity also reduces the efficiency of urea feed utilization in ruminants [44]. Enhancing the efficiency of urea-N conversion to rumen microbial-N has significant implications for ruminant nutrition, potentially improving protein synthesis and reducing nitrogen waste. In this study, we investigated the inhibitory effect of allicin on rumen microbial urease and its subsequent impact on in vitro rumen fermentation, microbial community composition, and urea nitrogen metabolic flux in dairy cows.

Our findings revealed that allicin inhibits rumen urease activity, leading to a reduced rate of urea hydrolysis. This effect was evident from the decrease in both Km and Vmax values with increasing allicin concentration, indicating that allicin exerts an anticompetitive inhibition on urease. Bacterial urease consists of structural genes *UreA*, *UreB*, and *UreC* encoding the α-subunit (UreC, which contains the active center), *β*-subunit (UreB), and *γ*-subunit (UreA), respectively [45–48]. Allicin was found to form hydrogen bonds with the amino acids in the active center of the *α*-subunit, which blocks the site for urea hydrolysis. This inhibition slowed the production of NH_3-N and increases microbial urea utilization, thus improving microbial protein synthesis [49]. Urease catalyzes urea by opening the flap region after urease is activated by nickel ions, allowing the substrate urea to enter the active center, which then displaces the three water molecules in the active site and closes the flap region when urea is bound to Ni^{+}. The inactivation of jack bean urease by allicin is caused by the reaction between allicin and the SH group located in the active site of urease (Cys^{592}) [47]. In this study, at the ruminal urease protein activity pocket UreC, allicin formed hydrogen bonds with ARG 1336 and Ni^{+}-linked molecule (H_2O^{373}), which occupied the urea attachment site and affected urease hydrolysis of urea. At the same time, urea could form hydrogen bonds with urease proteins ALA^{1224}, GLU^{1220}, and GLU^{1252} at UreC, forming a stable ternary complex (allicin-urease-urea). Enzyme inhibitors have three typical types of inhibition (competitive inhibition, noncompetitive inhibition, and anticompetitive inhibition), and parameters such as Km and the Vmax of the different types vary with the substrate concentration and enzyme concentration [48]. In this study, the kinetic data obtained in this study suggest that allicin may exert mixed-type inhibition on ruminal urease. While the observed decreases in both the Km and Vmax with increasing allicin concentration are consistent with anticompetitive inhibition (as reflected by the stable Km/Vmax ratio), molecular docking revealed a direct competitive interaction between allicin and urea for the active site of free UreC (via hydrogen bonds with ARG^{1336} and Ni^{2+}-linked H_2O^{373}). This contradiction implies a dual-binding mechanism:

- Competitive phase: Allicin initially competes with urea for the active site of free urease, increasing Km by reducing substrate accessibility.
- Uncompetitive phase: Allicin subsequently binds to the enzyme–substrate (urea-urease) complex, forming a stable ternary complex (allicin-urease-urea) that blocks product formation, thereby decreasing Vmax.

This two-stage model explains the concurrent reduction in Km and Vmax under low-substrate conditions. However, several critical experiments are required to validate this hypothesis:

- Kinetic assays with varying inhibitor-to-substrate ratios: To determine if the observed patterns deviate from pure competitive or uncompetitive inhibition
- Isotopic labelling studies: To identify whether allicin preferentially binds to free urease or the ES complex
- Structural analyses (e.g., cryo-electron microscopy): To visualize allicin interactions with both free and substrate-bound urease states.

(See figure on next page.)

Fig. 5 Metabolic flux of ^{15}N from $^{15}N^{15}N$-urea in rumen microorganisms. **A** Metabolites labelled with ^{15}N and their ^{15}N relative labelling ratio (conventional urea group background values were subtracted). Green indicates a ^{15}N relative labelling ratio > 50%, while pink indicates a ^{15}N relative labelling ratio > 30%, and gray indicates a relative ^{15}N labelling ratio < 30%. **B** The number and relative concentration of ^{15}N-labelled metabolites where the content of ^{15}N-labelled metabolite (M + 1/2/…) accounts for more than 30% of the total content of that metabolite (M + 0/1/2/…). M + 0 represents no ^{15}N labelling, and M + 1 represents one ^{15}N labelled, M + 2/3/…, and so on. The horizontal coordinate metabolite name is followed in parentheses by the number of nitrogen contained in one molecule of the substance. **C** Metabolic pathways involved in metabolites labelled with ^{15}N isotopes

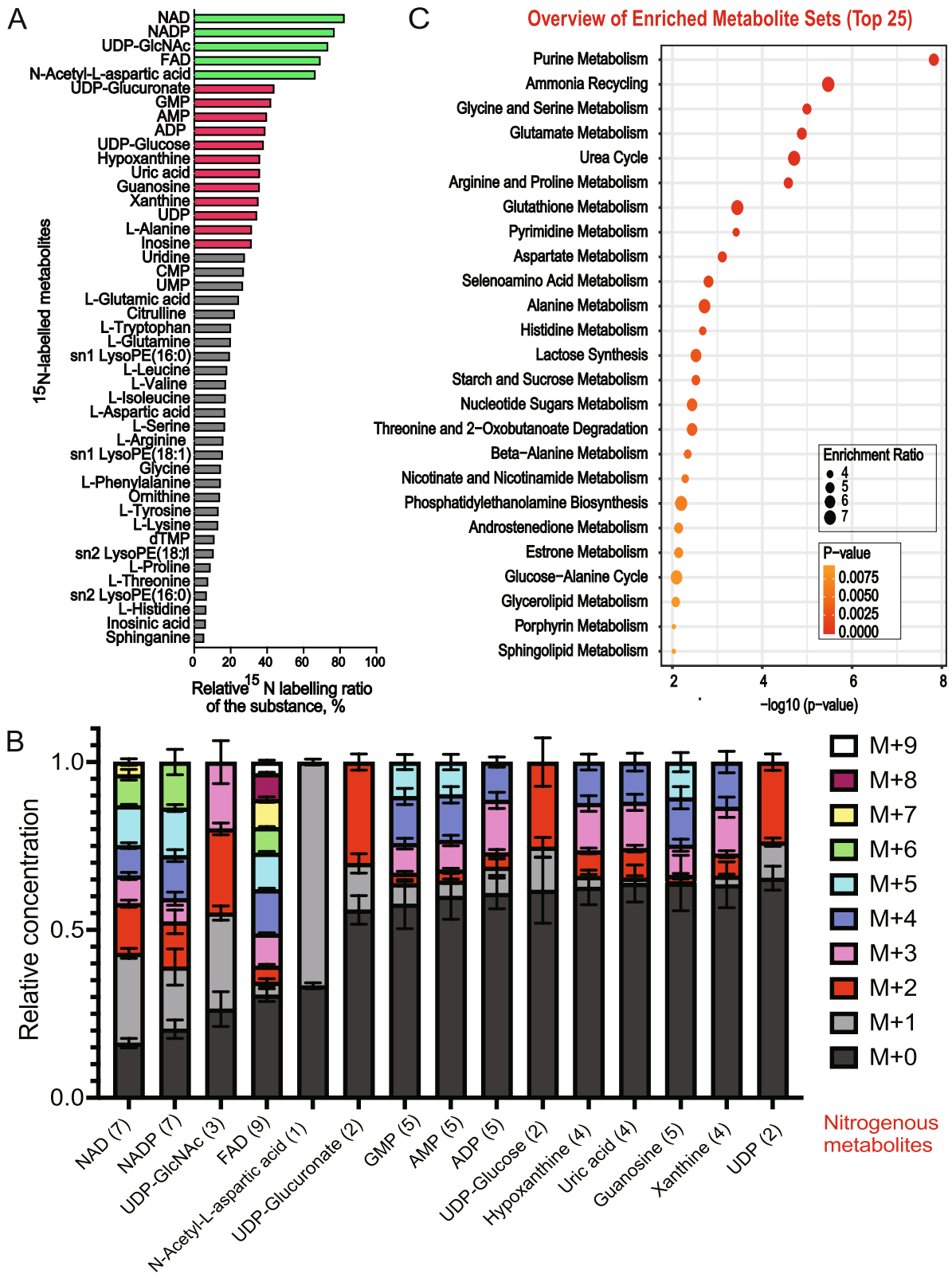

Fig. 5 (See legend on previous page.)

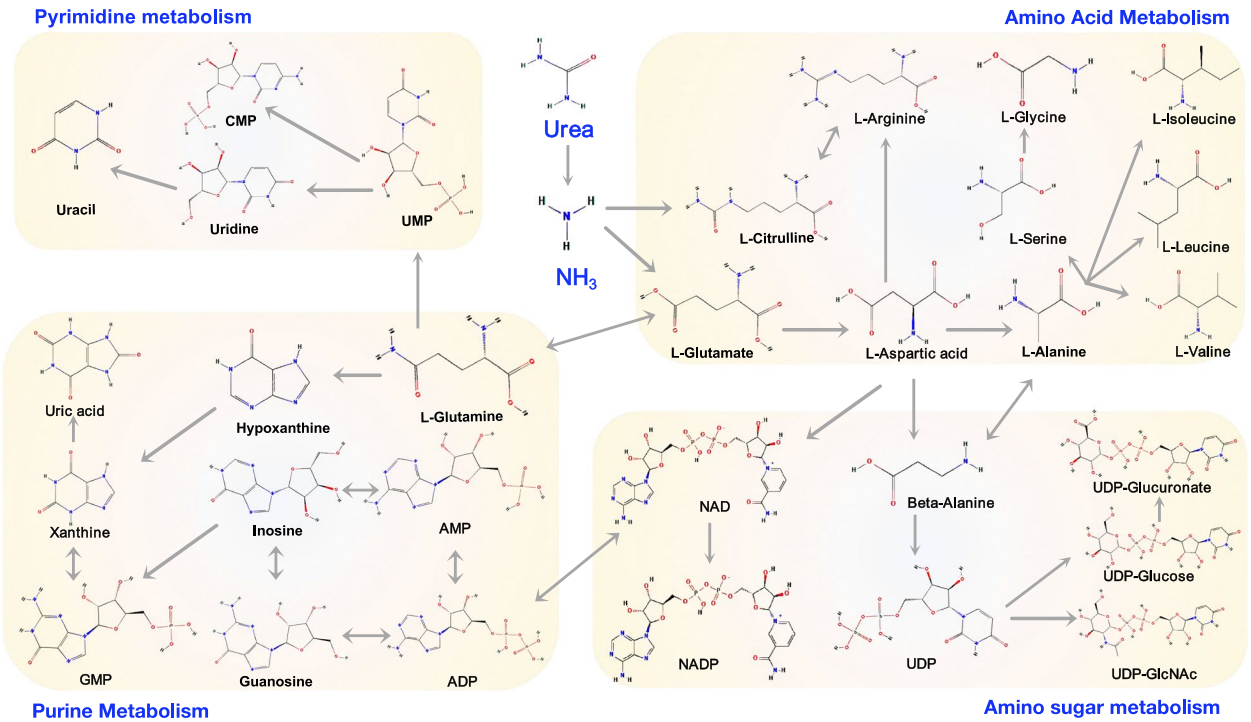

Fig. 6 Urea-N to microbial-N major metabolic pathways. AMP, adenosine 5′-monophosphate; GMP, guanosine 5′-monophosphate; NAD, nicotinamide adenine dinucleotide; NADP, nicotinamide adenine dinucleotide phosphate; UDP-GlcNAc, uridine diphosphate N-acetylglucosamine; UMP, uridine 5′-monophosphate

Our current data cannot definitively classify the inhibition type. Advanced functional assays, such as surface plasmon resonance to quantify inhibitor binding affinities for free and ES-bound urease, are essential to resolve this mechanistic ambiguity and advance our understanding of allicin's mode of action.

Beyond urease inhibition, allicin also modulates the rumen microbial community. Rumen microbes are the main finishers of rumen metabolism, and previous studies have demonstrated that allicin affects the composition of rumen microbes [50]. However, the mechanism by which allicin regulates the composition of rumen microorganisms is currently unknown. According to previous studies, allicin can regulate the growth of microorganisms by a variety of mechanisms such as altering the permeability of their cell membranes, inhibiting their enzyme activities, interfering with metabolic processes, and altering their genetic material [51, 52]. The effect of allicin on the mechanism of regulating the overall rumen microbial composition needs to be studied in depth. Notably, the reduction in the relative abundance of *Ruminococcus albus* and *Prevotella* sp. *R. albus* was demonstrated to be a ureolytic bacteria [53]. Consistently, garlic essential oil has been found to reduce the abundance of *R. albus* by Patra et al. [54]. It has been proven that *R. albus* is a urea-utilizing bacterium capable of growing with urea as the sole nitrogen source, which fully demonstrates that some species within the *R. albus* possess the ability to secrete urease. As a urease inhibitor, allicin may inhibit the growth of *R. albus* by suppressing the activity of the enzyme and thus limiting its nitrogen source utilization. Therefore, allicin may affect the growth of *R. albus*, reducing the secretion of urease and slowing down the degradation rate of urea.

Prevotella sp. are dominant genera of rumen microorganisms with the ability to degrade carbohydrates and proteins [55]. In particular, it is an important contribution to the deamination of peptides and amino acids [56, 57]. Allicin reduced the relative abundance of *Prevotella* sp. *(*MAG.45) in the rumen, which may be one of the reasons for increased urea nitrogen utilization by rumen microbes. *Prevotella* sp. (MAG.45) has an abundance of ammonia assimilation genes, including transaminases (*ROCD*, *ASPC*, *DAPL*), deaminases (*TADA*, *AGUA*, *ADE*, *GUAD*), peptidases (*DPP*, *PEPP*, *CTPA*, *PEPO*, *PEPD*), and amino acid de/transaminases (*ANSA*, *PYRB*, *LYSC*, *RPRX*). Reducing the population of *Prevotella* sp. reduces the amount of ammonia produced during amino acid and peptide degradation. Reduced ammonia from amino acid and small peptide sources in the rumen environment may have prompted rumen microbes to utilize ammonia produced from the degradation of urea nitrogen. This

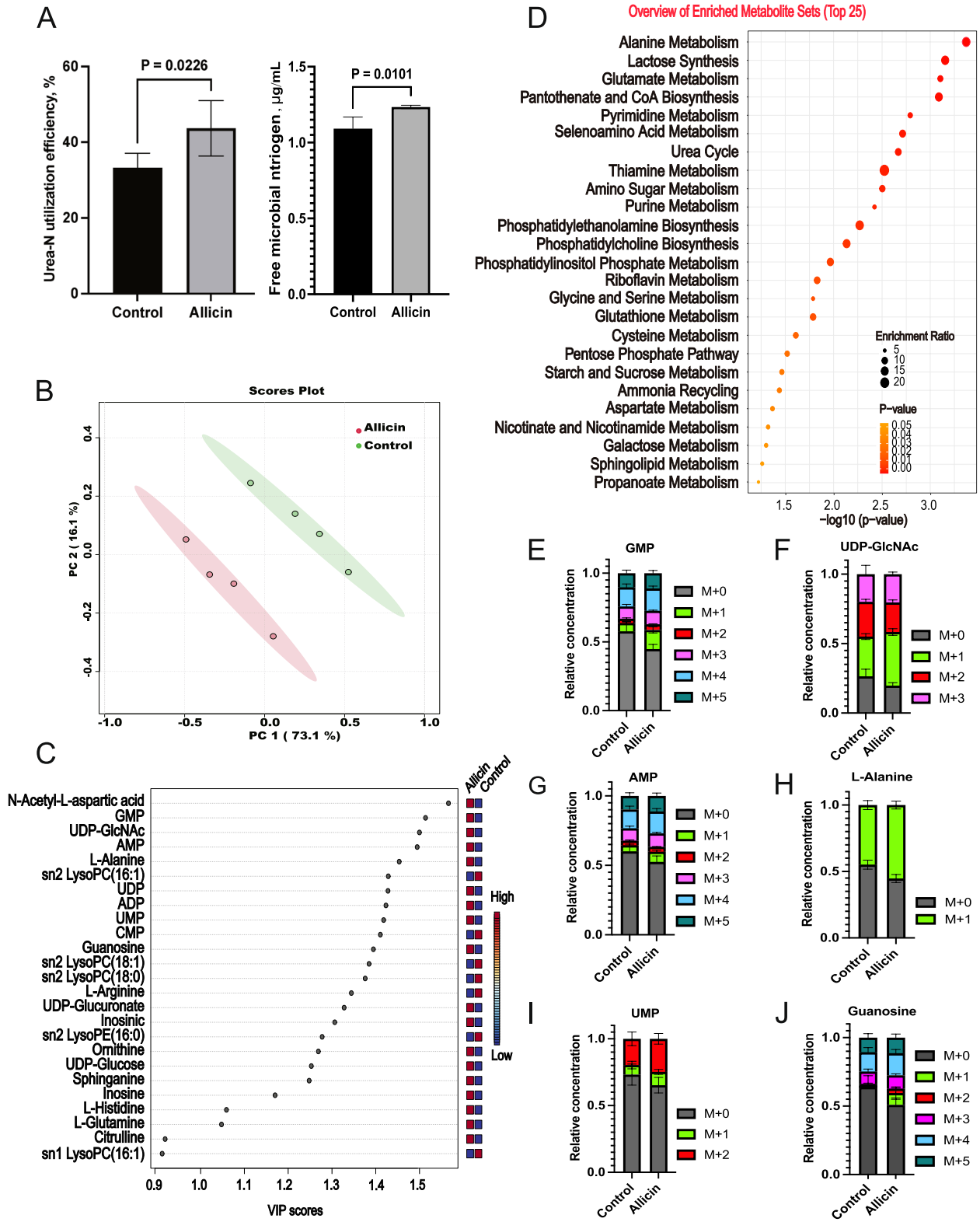

Fig. 7 Effect of allicin on urea-^{15}N metabolism. **A** Effect of allicin on the utilization of urea nitrogen by rumen microorganisms. **B** Principal component analysis scores plot of urea-N^{15} between the allicin (2 mM) group and control group. **C** The differential metabolites with VIP scores ≥ 1 by PLS-DA analysis. **D** The differential metabolites involving the top 25 metabolic pathways. **E**, **F**, **G**, **H**, **I**, **J** ^{15}N number and peak area information for major differential metabolites

implies that allicin may enhance the amount of peri-rumen amino acids and small peptides and does not reduce rumen microbial protein production, which is beneficial for ruminant nutrient digestion.

Metabolic flux analysis (MFA) is capable of revealing dynamic changes in metabolic pathways by quantifying the rates of metabolite production and consumption [58]. When studying the distribution of urea nitrogen in the rumen of ruminants, MFA can track the metabolic flux of urea nitrogen using isotopic labelling, identify key metabolic nodes and pathways, and provide theoretical support for optimizing urea nitrogen utilization efficiency and reducing nitrogen emissions. Our proposed metabolic pathways suggest that urea-N is hydrolyzed to NH_3-N and then participates in critical metabolic processes, including amino acid metabolism, purine metabolism, and amino sugar metabolism. These pathways are essential for the synthesis of microbial proteins, nucleotides, and other cellular components, underscoring the importance of efficient nitrogen utilization in rumen microbial growth and activity. Amino acid metabolism plays a crucial role in the synthesis of microbial proteins, which are an important source of dietary proteins for host ruminants [59]. Purine metabolism contributes to the production of nucleotides, which are important components of DNA and RNA responsible for microbial growth and proliferation [60]. Amino acid gluconeogenesis emphasizes its role in the biosynthesis of important cellular components such as glycoproteins, glycolipids, and peptidoglycans [61]. The proposed metabolic pathways and transformation processes of urea in rumen microorganisms highlight the importance of urea in the formation of nitrogen utilization and microbial activity in the rumen ecosystem.

Allicin's enhancement of urea nitrogen utilization is further supported by the increased relative abundance of *D. detoxificans* involved in nitro compound metabolism, respectively. *D. detoxificans*, known for metabolizing nitro compounds, may also play a role in reducing methane production in the rumen, as supported by previous studies [62–64]. Noticeably, *D. detoxificans* also has a peptidase gene (*FRVX*), an amino acid ABC transporter gene (*TCYB*), an aspartate transaminase gene (*PYRB*), an aminotransferase gene (*ALATA*), a glutamine synthetase gene (*GLNA*), and a gene for hydrolysis of glutamine to glutamate and ammonia (*PDXT*). Capable of complete nitrogen utilization cycle. Thus, the increase in relative abundance of *D. detoxificans* may also be another factor in the increased urea nitrogen utilization by allicin.

In this study, the DMSO concentration was carefully controlled at 0.1% in each 65-mL culture system, which is below the threshold (0.5–1%) where significant inhibitory effects on bacterial growth are observed [65–68]. This approach minimized the potential impact of DMSO on rumen urea nitrogen metabolism and ensured that any observed effects were primarily due to the tested compounds rather than the solvent. The rumen simulation system is a widely used experimental method in ruminant nutrition research. Compared to animal trials, it offers several advantages, including simplicity, lower cost, faster results, and no animal welfare concerns. It has been recommended in numerous review articles as an excellent tool for rumen simulation studies [69, 70]. This system is not only used to determine ruminal degradation rates of feed but also to simulate nitrogen metabolism by rumen microbes. The anaerobic conditions maintained within this system ensure the proper growth of rumen microbes, enabling normal fermentation and reliable nitrogen metabolism simulation. However, as this study employed a batch culture system, future studies could benefit from using continuous culture systems or fistulated animals to validate the effects of allicin. This approach would provide more robust insights for guiding the development of new feed additives.

Allicin significantly enhances ruminant health and productivity by improving rumen microbial diversity and modulating the microbiome to foster a more efficient and healthy rumen ecosystem. This discovery not only provides a novel regulatory strategy for the ruminant feeding industry but also provides strong support for achieving green and efficient development in agricultural production. While our findings highlight the potential benefits of allicin treatment on microbial diversity, it is essential to consider the potential long-term ecological risks associated with these changes. The emergence of less dominant microbial species, as observed with allicin treatment, could impact the stability of the rumen ecosystem. Although increased abundance of *Ruminobacter* and *RC9* may enhance specific metabolic functions, the long-term consequences of these shifts remain unclear. Long-term monitoring is essential to assess their impact on rumen health and animal performance. Minor shifts in microbial communities can significantly alter ecosystem function, especially when the balance between dominant and less dominant species is disrupted. Future research should focus on long-term studies to evaluate the stability and resilience of the rumen microbiome under continuous allicin treatment. This will provide insights into its long-term effects on rumen health and nutrient utilization. Beyond the rumen, changes in microbial diversity could have broader ecological implications, such as altering greenhouse gas emissions and digestive efficiency. While allicin treatment may improve fiber degradation and nitrogen fixation, it could also affect methane production and other fermentation by-products. Balancing enhanced

nutrient utilization with ecological stability is crucial for sustainable ruminant production.

Conclusions

In summary, allicin exerts an inhibitory effect on rumen urease activity, reducing the rapid hydrolysis of urea and enhancing the efficiency of urea nitrogen utilization. By modulating the rumen microbial community, allicin promotes microbial protein synthesis and amino acid metabolism. These findings highlight the therapeutic potential of allicin as a urease inhibitor and suggest that urea feeds play a crucial role in supporting rumen microbial metabolism and protein synthesis. Furthermore, our finding that urea nitrogen is involved in important life processes such as rumen microbial amino acid, purine, and pyrimidine metabolism indicated the important nutritional function of urea feeds for rumen metabolism and microbial protein synthesis. Future research should explore the in vivo application of allicin as a feed additive in ruminant nutrition to fully investigate its benefits on production performance, growth metabolism, and livestock product quality.

Abbreviations

AMP	Adenosine 5′-monophosphate
DMSO	Dimethyl sulfoxide
PCA	Principal component analysis
PLS-DA	Partial least squares discriminant analysis
GMP	Guanosine 5′-monophosphate
HEPES	4-Hydroxyethyl piperazine ethane sulfonic acid
NAD	Nicotinamide adenine dinucleotide
NADP	Nicotinamide adenine dinucleotide phosphate
PBS	Phosphate buffer saline
UDP-GlcNAc	Uridine diphosphate N-acetylglucosamine
UMP	Uridine 5′-monophosphate
VFAs	Volatile fatty acids

Supplementary Information

The online version contains supplementary material available at https://doi.org/10.1186/s40168-025-02111-z.

Additional file 1: Supplemental Table 1. Allicin, urea, and homologous modelling protein molecular docking parameters.

Additional file 2: Supplemental Table 2. Genomic information.

Acknowledgements

We express our gratitude to the dairy farm belonging to IAS for their efforts in collecting rumen fluid from lactating dairy cows.

Authors' contributions

SGZ and SQZ designed the experiment. JQW, SQZ and SGZ gave funding support. SQZ performed enzymatic kinetic analyses, fermentation index measurements, microbial cultures, DNA extraction and metabolic flux analyses. SGZ performed genome sequencing and conducted the bioinformatic analysis. SQZ uploaded all the data to the database. SQZ and SGZ performed all the statistical analysis and figures generation. SQZ and SGZ wrote the manuscript. JQW and NZ gave suggestions for manuscript revision. The authors read and approved the final manuscript.

Funding

This work was supported by the National Key R&D Program of China (2022YFD1301000), the Project Funded by China Postdoctoral Science Foundation under Grant Number 2023M743835, the Agricultural Science and Technology Innovation Program (CAAS-ZDRW202308), and the State Key Laboratory of Animal Nutrition and Feeding (2004DA125184G2406).

Data availability

The macrogenome sequence has been deposited in the National Microbiology Data Centre of China (https://nmdc.cn/en) under the accession number NMDC10019225.

Declarations

Ethics approval and consent to participate

All experimental procedures involving dairy cows were approved by the Animal Care and Use Committee for Livestock of the Institute of Animal Sciences, Chinese Academy of Agricultural Sciences (No. IAS201914).

Consent for publication

Not applicable.

Competing interests

The authors declare no competing interests.

Received: 4 September 2024 Accepted: 11 April 2025
Published online: 16 May 2025

References

1. Poore J, Nemecek T. Reducing food's environmental impacts through producers and consumers. Science. 2018;360(6392):987–92.
2. Guerrero AM, Jones NA, Ross H, Virah-Sawmy M, Biggs D. What influences and inhibits reduction of deforestation in the soy supply chain? A mental model perspective. Environ Sci Policy. 2021;115:125–32.
3. Ghelichkhan M, Eun JS, Christensen RG, Stott RD, MacAdam JW. Urine volume and nitrogen excretion are altered by feeding birdsfoot trefoil compared with alfalfa in lactating dairy cows1. J Anim Sci. 2018;96(9):3993–4001.
4. Wilson RL, Bionaz M, MacAdam JW, Beauchemin KA, Naumann HD, Ates S. Milk production, nitrogen utilization, and methane emissions of dairy cows grazing grass, forb, and legume-based pastures. J Anim Sci. 2020;98(7):skaa220.
5. Kuoppala K, Jaakkola S, Garry B, Ahvenjärvi S, Rinne M. Effects of faba bean, blue lupin and rapeseed meal supplementation on nitrogen digestion and utilization of dairy cows fed grass silage-based diets. Animal. 2021;15(7): 100300.
6. Fagundes MA, Hall JO, Eun JS. Effects of feeding different forms of lysine supplements on lactational performance and nitrogen utilization by mid- to late-lactation dairy cows. Appl Anim Sci. 2022;38(1):1–12.
7. Sweeny JP, Surridge V, Humphry PS, Pugh H, Mamo K. Benefits of different urea supplementation methods on the production performances of Merino sheep. Vet J. 2014;200(3):398–403.
8. Jin D, Zhao SG, Zheng N, Bu DP, Beckers Y, Wang JQ. Urea nitrogen induces changes in rumen microbial and host metabolic profiles in dairy cows. Livest Sci. 2018;210:104–10.
9. Pereira GA, Oliveira JS, Santos EM, Carvalho GGP, Araújo GGL, Sousa WH, Neto SD, Cartaxo FQ. Substitution of soybean meal for urea in diets based on deferred buffelgrass hay for feedlot sheep. Rev Bras Zootecn. 2018;47: e20170035.
10. Wickersham TA, Titgemeyer EC, Cochran RC, Gnad DP. Effect of rumen-degradable intake protein supplementation on urea kinetics and microbial use of recycled urea in steers consuming low-quality forage. J Anim Sci. 2008;86(11):3079–88.
11. Bach A, Calsamiglia S, Stern MD. Nitrogen metabolism in the rumen. J Dairy Sci. 2005;88(Suppl 1):E9–21.
12. Hristov AN, Oh J, Lee C, Meinen R, Montes F, Ott T, Firkins J, Rotz A, Dell C, Adesogan A, et al. Mitigation of greenhouse gas emissions in livestock

production – a review of technical options for non-CO_2 emissions. 2013; Rome, Italy: FAO.
13. Patra AK, Aschenbach JR. Ureases in the gastrointestinal tracts of ruminant and monogastric animals and their implication in urea-N/ammonia metabolism: a review. J Adv Res. 2018;13:39–50.
14. Zhu Z, Mao S, Zhu W. Effects of ruminal infusion of garlic oil on fermentation dynamics, fatty acid profile and abundance of bacteria involved in biohydrogenation in rumen of goats. Asian-Australas J Anim Sci. 2012;25(7):962–70.
15. Ahmed E, Batbekh B, Fukuma N, Kand D, Nishida T. A garlic and citrus extract: impacts on behavior, feed intake, rumen fermentation, and digestibility in sheep. Anim Feed Sci Tech. 2021;278(4): 115007.
16. Mathialagan R, Mansor N, Al-Khateeb B, Mohamad MH, Shamsuddin MR. Evaluation of allicin as soil urease inhibitor. Procedia Eng. 2017;184:449–59.
17. Salehuddin NF, Mansor N, Yahya WZN, Affendi NM. Organosulfur compounds as soil urease inhibitors and their effect on kinetics of urea hydrolysis. J Soil Sci Plant Nut. 2021;21:2652–9.
18. Zhao SG, Wang JQ, Bu DP, Zhou LY, Sun P. Effect of plant essential oil on the distribution of urea-nitrogen in rumen contents. Chinese Agricultural Science. 2012;16:3399–405 (in Chinese).
19. Carter EL, Flugga N, Boer JL, Mulrooney SB, Hausinger RP. Interplay of metal ions and urease. Metallomics. 2009;1(3):207–21.
20. Li C, Huang P, Wong K, Tan L, Chen H, Lu Q, Luo C, Tam C, Zhu L, Su Z, et al. Coptisine-induced inhibition of Helicobacter pylori: elucidation of specific mechanisms by probing urease active site and its maturation process. J Enzyme Inhib Med Chem. 2018;33(1):1362–75.
21. Zhao Y, Shi R, Bian X, Zhou C, Zhao Y, Zhang S, Wu F, Geoffrey IW, Wu L, Tung C, et al. Ammonia detection methods in photocatalytic and electrocatalytic experiments: how to improve the reliability of NH_3 production rates? Adv Sci. 2019;6(8):1802109.
22. He Y, Zhang X, Li M, Zheng N, Zhao S, Wang J. Coptisine: A natural plant inhibitor of ruminal bacterial urease screened by molecular docking. Sci Total Environ. 2022;808: 151946.
23. Zhang X, Zhao S, He Y, Zheng N, Yan X, Wang J. Substitution of residues in UreG to investigate UreE interactions and nickel binding in a predominant urease gene cluster from the ruminal metagenome. Int J Biol Macromol. 2020;161:1591–601.
24. Menke KH, Steingass H. Estimation of the energetic feed value obtained from chemical analysis and in vitro gas production using rumen fluid. Anim Res Dev. 1988;28:7–55.
25. Liu S, Zhang Z, Hailemariam S, Zheng N, Wang M, Zhao S, Wang J. Biochanin a inhibits ruminal nitrogen-metabolizing bacteria and alleviates the decomposition of amino acids and urea *in vitro*. Animals (Basel). 2020;10(3):368.
26. Behan AA, Loh TC, Fakurazi S, Kaka U, Kaka A, Samsudin AA. Effects of supplementation of rumen protected fats on rumen ecology and digestibility of nutrients in sheep. Animals (Basel). 2019;9(7):400.
27. Broderick GA, Kang JH. Automated simultaneous determination of ammonia and total amino acids in ruminal fluid and in vitro media. J Dairy Sci. 1980;63(1):64–75. https://doi.org/10.3168/jds.S0022-0302(80)82888-8.
28. Minas K, McEwan NR, Newbold CJ, Scott KP. Optimization of a high-throughput CTAB-based protocol for the extraction of qPCR-grade DNA from rumen fluid, plant and bacterial pure cultures. FEMS Microbiol Lett. 2011;325(2):162–9.
29. Mehdipour P, Marhon SA, Ettayebi I. Epigenetic therapy induces transcription of inverted SINEs and ADAR1 dependency. Nature. 2020;588(7836):169–73.
30. Uritskiy GV, DiRuggiero J, Taylor J. MetaWRAP-a flexible pipeline for genome-resolved metagenomic data analysis. Microbiome. 2018;6(1):158.
31. Kopylova E, Noé L, Touzet H. SortMeRNA: fast and accurate filtering of ribosomal RNAs in metatranscriptomic data. Bioinformatics. 2012;28(24):3211–7.
32. Waschulin V, Borsetto C, James R, Newsham KK, Donadio S, Corre C, Wellington E. Biosynthetic potential of uncultured Antarctic soil bacteria revealed through long-read metagenomic sequencing. ISME J. 2022;16(1):101–11.
33. Li D, Liu CM, Luo R, Sadakane K, Lam TW. MEGAHIT: an ultra-fast single-node solution for large and complex metagenomics assembly via succinct de Bruijn graph. Bioinformatics. 2015;31(10):1674–6.
34. Parks DH, Imelfort M, Skennerton CT, Hugenholtz P, Tyson GW. CheckM: assessing the quality of microbial genomes recovered from isolates, single cells, and metagenomes. Genome Res. 2015;25(7):1043–55.
35. Parks DH, Rinke C, Chuvochina M, Chaumeil P, Woodcroft B, Evans PN, Hugenholtz P, Tyson GW. Recovery of nearly 8,000 metagenome-assembled genomes substantially expands the tree of life. Nat Microbiol. 2017;2(11):1533–42.
36. Hyatt D, Chen GL, Locascio PF, Land ML, Larimer FW, Hauser LJ. Prodigal: prokaryotic gene recognition and translation initiation site identification. BMC Bioinformatics. 2010;11:119.
37. Huerta-Cepas J, Szklarczyk D, Heller D, Hernández-Plaza A, Forslund SK, Cook H, Mende DR, Letunic I, Rattei T, Jensen LJ, et al. eggNOG 5.0: a hierarchical, functionally and phylogenetically annotated orthology resource based on 5090 organisms and 2502 viruses. Nucleic Acids Res. 2019;47(D1):D309–14.
38. Chong J, Liu P, Zhou G, Xia J. Using MicrobiomeAnalyst for comprehensive statistical, functional, and meta-analysis of microbiome data. Nat Protoc. 2020;15(3):799–821.
39. Pang Z, Chong J, Zhou G, de Lima Morais DA, Chang L, Barrette M, Gauthier C, Jacques PÉ, Li S, Xia J. MetaboAnalyst 5.0: narrowing the gap between raw spectra and functional insights. Nucleic Acids Res. 2021;49(W1):W388–96.
40. Shen L, Hu P, Zhang Y, Ji Z, Shan X, Ni L, Ning N, Wang J, Tian H, Shui G, et al. Serine metabolism antagonizes antiviral innate immunity by preventing ATP6V0d2-mediated YAP lysosomal degradation. Cell Metab. 2021;33(5):971–87.
41. Zimmermann M, Sauer U, Zamboni N. Quantification and mass isotopomer profiling of α-keto acids in central carbon metabolism. Anal Chem. 2014;86(6):3232–7.
42. Song JW, Lam SM, Fan X, Cao WJ, Wang SY, Tian H, Chua GH, Zhang C, Meng FP, Xu Z, et al. Omics-driven systems interrogation of metabolic dysregulation in COVID-19 pathogenesis. Cell Metab. 2020;32(2):188–202.
43. Tian H, Ni Z, Lam SM, Jiang W, Li F, Du J, Wang Y, Shui G. Precise metabolomics reveals a diversity of aging-associated metabolic features. Small Methods. 2022;6(7): e2200130.
44. Lopes ASM, de Oliveira JS, Santos EM, Medeiros AN, Givisiez PEN, Lemos MLP. Goats fed with non-protein nitrogen: ruminal bacterial community and ruminal fermentation, intake, digestibility and nitrogen balance. J Agric Sci. 2020;158(8–9):781–90.
45. Zambelli B, Musiani F, Benini S, Ciurli S. Chemistry of Ni^{2+} in urease: sensing, trafficking, and catalysis. Acc Chem Res. 2011;44(7):520–30.
46. Kappaun K, Piovesan AR, Carlini CR, Ligabue-Braun R. Ureases: historical aspects, catalytic, and non-catalytic properties - a review. J Adv Res. 2018;13:3–17.
47. Juszkiewicz A, Zaborska W, Sepioł J, Góra M, Zaborska A. Inactivation of jack bean urease by allicin. J Enzyme Inhib Med Chem. 2003;18(5):419–24.
48. Whiteley CG. Enzyme kinetics: partial and complete non-competitive inhibition. Biochemical Education. 1999;28:144–7.
49. Calsamiglia S, Cardozo PW, Ferret A, Bach A. Changes in rumen microbial fermentation are due to a combined effect of type of diet and pH. J Anim Sci. 2008;86(3):702–11.
50. Liu TW, Pang R, Huang L, Mao TT, Yu JJ, Hua JL, Zhong YF, Ren CH, Zhang ZJ, Zhu W. Effects of allicin addition on growth performance, rumen microbiome, and ruminal epithelial proteome of high-grain-fed goats. Anim Feed Sci Tech. 2024;310: 115944.
51. Müller A, Eller J, Albrecht F, Prochnow P, Kuhlmann K, Bandow JE, Slusarenko AJ, Leichert LI. Allicin induces thiol stress in bacteria through S-allylmercapto modification of protein cysteines. J Biol Chem. 2016;291(22):11477–90.
52. Rabinkov A, Miron T, Konstantinovski L, Wilchek M, Mirelman D, Weiner L. The mode of action of allicin: trapping of radicals and interaction with thiol containing proteins. Biochim Biophys Acta. 1998;1379(2):233–44.
53. Seshadri R, Leahy SC, Attwood GT, Teh KH, Lambie SC, Cookson AL, Eloe-Fadrosh EA, Pavlopoulos GA, Hadjithomas M, Varghese NJ, et al. Cultivation and sequencing of rumen microbiome members from the Hungate1000 Collection. Nat Biotechnol. 2018;36(4):359–67.

54. Patra AK, Yu Z. Effects of essential oils on methane production and fermentation by, and abundance and diversity of, rumen microbial populations. Appl Environ Microbiol. 2012;78(12):4271–80.
55. Stevenson DM, Weimer PJ. Dominance of Prevotella and low abundance of classical ruminal bacterial species in the bovine rumen revealed by relative quantification real-time PCR. Appl Microbiol Biotechnol. 2007;75(1):165–74.
56. Wang ZB, Xin H, Bao J, Duan C, Chen Y, Qu Y. Effects of hainanmycin or monensin supplementation on ruminal protein metabolism and populations of proteolytic bacteria in Holstein heifers. Anim Feed Sci Tech. 2015;201:99–103.
57. Ferme D, Banjac M, Calsamiglia S, Busquet M, Kamel C, Avgustin G. The effects of plant extracts on microbial community structure in a rumen-simulating continuous-culture system as revealed by molecular profiling. Folia Microbiol. 2004;49(2):151–5.
58. Moiz B, Sriram G, Clyne AM. Interpreting metabolic complexity via isotope-assisted metabolic flux analysis. Trends Biochem Sci. 2023;48(6):553–67.
59. Dora Z, Kristina K, Jasna A. Metabolism and utilisation of non-protein nitrogen compounds in ruminants: a review. Journal of Central European Agriculture. 2023;24(1):1–14.
60. Kasahara K, Kerby RL, Zhang Q, Pradhan M, Mehrabian M, Lusis AJ, Bergström G, Bäckhed F, Rey FE. Gut bacterial metabolism contributes to host global purine homeostasis. Cell Host Microbe. 2023;31(6):1038-1053.e10.
61. Ling ZN, Jiang YF, Ru JN, Lu JH, Ding B, Wu J. Amino acid metabolism in health and disease. Signal Transduct Target Ther. 2023;8(1):345.
62. Anderson RC, Rasmussen MA, Jensen NS, Allison MJ. Denitrobacterium detoxificans gen. nov., sp. nov., a ruminal bacterium that respires on nitrocompounds. Int J Syst Evol Microbiol. 2000;50(Pt 2):633–8.
63. Busquet M, Calsamiglia S, Ferret A, Carro MD, Kamel C. Effect of garlic oil and four of its compounds on rumen microbial fermentation. J Dairy Sci. 2005;88(12):4393–404.
64. Ma T, Chen D, Tu Y, Zhang N, Si B, Deng K, Diao Q. Effect of supplementation of allicin on methanogenesis and ruminal microbial flora in Dorper crossbred ewes. J Anim Sci Biotechnol. 2016;7:1.
65. Jessup CJ, Warner J, Isham N, Hasan I, Ghannoum MA. Antifungal susceptibility testing of dermatophytes: establishing a medium for inducing conidial growth and evaluation of susceptibility of clinical isolates. J Clin Microbiol. 2000;38(1):341–4.
66. Randhawa MA. The effect of dimethyl sulfoxide (DMSO) on the growth of dermatophytes. Nippon Ishinkin Gakkai Zasshi. 2006;47(4):313–8.
67. Kirkwood ZI, Millar BC, Downey DG, Moore JE. Antimicrobial effect of dimethyl sulfoxide and N, N-dimethylformamide on Mycobacterium abscessus: implications for antimicrobial susceptibility testing. Int J Mycobacteriol. 2018;7(2):134–6.
68. Chang XJ, Xu YC, Liu C. Effects of common organic solvents on bacterial activity and their safe use limits detected by different experimental methods. Microbiology Bulletin. 2016;07:1635–45 (in Chinese).
69. Deitmers J, Gresner N, Südekum K. Opportunities and limitations of a standardisation of the rumen simulation technique (RUSITEC) for analyses of ruminal nutrient degradation and fermentation and on microbial community characteristics. Anim Feed Sci Technol. 2022;289: 115325.
70. Tan J, Wang Y, Niu H, Li L, Zhao H, Fang L, Jiang L, Zhao Y. Metagenomic insights into the mechanistic differences of plant polyphenols and nitrocompounds in reducing methane emissions using the rumen simulation technique. Sci Total Environ. 2024;953: 176135.

Publisher's Note